Synchrotron fibre diffraction identifies and locates foetal collagenous breast tissue associated with breast carcinoma

Veronica J. James

Research School of Chemistry, Australian National University, Canberra, Australia, School of Physics, The University of Sydney, Sydney, Australia, and Department of Pathology, University of Western Australia, Nedlands, Perth, Australia. E-mail: vjs@bigpond.com

Synchrotron fibre diffraction studies of collagenous breast tissue have revealed clear and consistent differences in the diffraction intensity patterns between samples taken from patients with breast carcinoma and those taken from controls. These changes, prelusive to carcinoma, are related to changes in and breakdown of the molecular structure of the collagen type IV support collagen adjacent to the type I, type III and type V collagen fibrils. In order to locate the positions and sequence of the different molecular arrangements, multiple samples were taken from a number of patients. The first of these was taken as near to the tumour site as was possible. Subsequent samples were taken at intervals along ducts leading away from the tumour. The results reveal that the collagen distal from the tumour is similar to that of the controls and this was taken as the standard molecular structure of breast tissue. It usually contained some fat. For normal samples taken closer to the tumour site, the wide diffraction ring associated with fat disappears leaving only the fibrillar pattern. Moving closer to the tumour a 'foetal-like tissue' was observed. The tissue immediately adjacent to the tumour was found to have the same molecular structure as that of foetal tissue.

Keywords: fibre diffraction; foetal collagen; breast cancer.

1. Introduction

Fibre diffraction has been greatly enhanced by the very bright finely focused beams of synchrotrons. Weak changes, not visible in conventional X-ray diffraction studies, are clearly seen even with greatly reduced exposure times. Using this technique, James *et al.* (1998) have determined the molecular structure of primordial embryonic foetal tendon and skin, using human foetal samples within an age range of 15–18 weeks from conception. This study revealed a normal fibrillar pattern for skin for both tissues which was superimposed by a large number of orders of a 353 nm lattice which relates to the branching network of collagen type IV in the connective tissue. Details of this weak superimposed signal and the methods used to ensure its validity are given by James *et al.* (1993*b*). While electron and light microscopy have been used to study these stromal tissues, synchrotron fibre diffraction studies can extend knowledge to a molecular level, with a focus small enough to examine the same sample at a number of different locations. In addition, X-ray diffraction offers a good 'bulk averaged' picture of the molecular changes taking place at the region of interest in a particular sample. Fibre diffraction is also non-invasive and the samples can be used for further studies by other techniques.

In normal dermal breast tissue, the collagen fibrils are embedded in fat and closely grouped immediately adjacent and parallel to the lobules and ducts in the stroma (the connective tissue that forms the framework of the breast). Such a pseudocrystalline arrangement is ideal for fibre diffraction studies. Histopathology slides from breast biopsies, specifically stained for collagen, reveal that the fibrillar nature of the ductal stroma immediately adjacent to ducts is often replaced by what is known as hyalinized collagenous tissue in and sometimes preceding breast carcinoma. Hyalinized collagenous tissue appears to have no normal fibrous structure on a histopathology slide, as can be seen in Fig. 1, where the two large ducts seen in cross-section in the central section are surrounded by hyalinized collagen (the 'flat' areas). The presence of such hyalinized tissue evidenced on histopathology slides from mastectomy sections is often referred to as the presence of periductal elastosis.

Normal fibrillar collagen is visible in the connective tissue located between these two hyalinized areas in Fig. 1. When viewed with a polarizing microscope, it is seen that there is almost no fat remaining in the hyalinized tissue but is certainly present in the area occupied by the fibrillar collagen. Normally, however, only one large duct can be

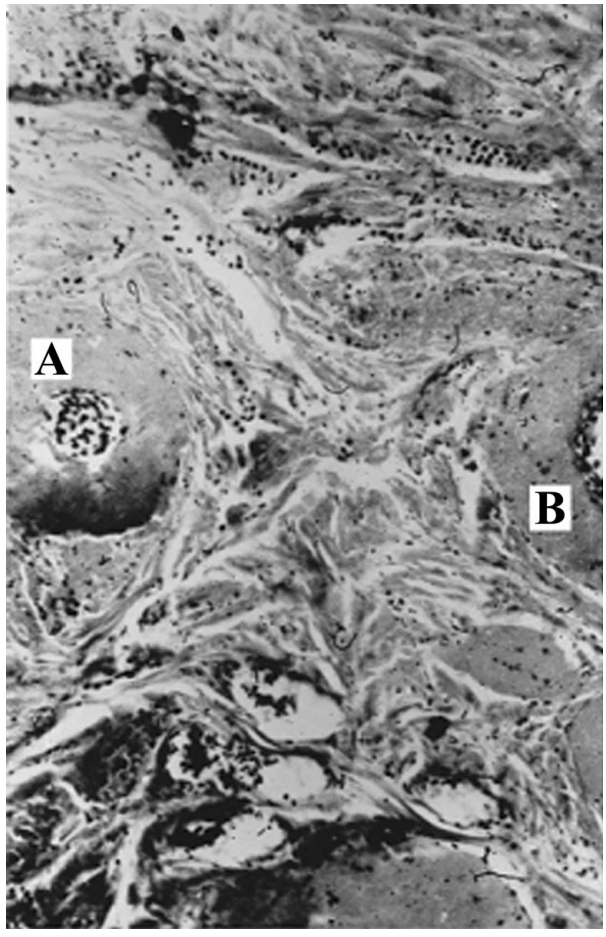

Figure 1
This histopathology slide was created from tissue removed during a mastectomy, and specifically stained for collagen. When viewed with a light microscope, two large ducts, A and B, are visible in the central section. There is no cancer in these ducts. The specific staining reveals that the 'flat' areas surrounding these ducts which appear to contain no fibrous collagenous material are actually hyalinized collagenous tissue. The tissue in these hyalinized sections is extremely dense; in fact, a hypodermic needle will bend rather than pass through it. There is almost no fat in these flattened areas and, as a result of this, the two large ducts are drawn abnormally close to each other. Between these two areas of very dense hyalinized collagenous tissue is an area of normal fibrous stroma. At the bottom of the slide, ductal carcinoma is revealed within a third duct and this duct is also surrounded by hyalinized tissue.

seen on any histopathology slide but, in this case, the loss of fatty tissue from the hyalinized areas causes a void which draws the two ducts abnormally close to each other so that they are visible on the same section. There is no carcinoma in these ducts at this time and so these changes are themselves a prelude to pathological change, that is a proemial change for breast cancer. Histopathology indicates that ductal carcinoma starts and proliferates in the epithelial layer on the surface of ducts within the hyalinized regions. Evidence of this can be seen in the cancerous masses in the large duct at the bottom of the slide. An understanding of the aetiology† of these proemial structural changes in the collagen of the ductal and lobular regions in breast carcinoma is therefore vital to understanding the origins of the carcinoma itself. This study was set up to investigate the nature and sequence of these changes.

2. Materials and method

210 samples of breast tissue, from patients aged between 30 and 85, were used for this investigation. These included tissue from eight cases of invasive ductal carcinoma, 22 cases of intraductal carcinoma, 13 cases of infiltrating lobular carcinoma, 61 ductal tissue samples adjacent to the carcinoma and 39 ductal tissue samples distal from the carcinoma which appeared to be normal tissue as determined either by eye or histopathology. In addition, 67 'normal' ducts were obtained either at autopsy, from proliferative fibrocystic change or from normal tissue biopsies of the breast. Sections of duct were chosen so that the fibrillar collagen would be preferentially aligned parallel to the surface of the duct.

Although only one sample was obtained for most patients, two to five samples were taken from each of 30 patients, later diagnosed with either ductal or lobular carcinoma (74 samples in total). The first samples in such cases were taken from sections of ducts either containing cancerous tissue or sections of ducts in the periductal or interlobular stroma as near as possible to the carcinoma. When possible, successive samples were taken moving along these ducts away from the cancer site until the final distal sample appeared to be normal tissue.

The samples were typically 1 mm wide and 10 mm long after removal of approximately 1 mm from each end for the histopathology. After removal, the samples were placed immediately in physiological saline and stored at 253 K until required. During the experiment the samples were maintained at 100% humidity in specially constructed cells. These cells are also designed to allow the samples to be stretched slightly to remove the natural crimp, thus improving the diffraction patterns.

The fibre diffraction experiments were carried out on the beamline 15A facility at the Photon Factory, Tsukuba, Japan (James *et al.*, 1993*a*). Samples were investigated using sample-to-detector distances of 600 and 2400 mm with exposure times of 5 to 60 s. Data were recorded on FUJI BAS imaging plates and later extracted by electronic scan. Calibration was achieved by comparison with diffraction patterns from moist rat-tail tendon, assumed to have a *D*-spacing of 67 nm.

A high-precision analysis of the two dimensional data was carried out using the astronomy computing packages *IRAF* (IRAF Programming Group, 1986) and *SAO Image* (Van Hilst, 1990). The positions and intensities of the reflections were determined by four different methods, namely (i) directly from the image after the background had been fitted with a boxcar average and removed from the original image, (ii) directly from an intensity plot of the background-corrected data, (iii) scanning with a mouse over the raw data and (iv) peak location using a second-order derivative plot of data previously smoothed by the application of best-fit Legendre polynomials. The inner equatorial reflections were fitted to cylindrical arrays using a first-order cylindrical Bessel function analysis. A typical low-angle diffraction pattern of normal breast tissue taken with a 2400 mm camera length is shown in Fig. 2. These results were subsequently confirmed at the BioCAT facility at the Advanced Photon Source, Argonne National Laboratory, USA.

All experiments and procedures had been approved by the appropriate Ethics Review Committees of the synchrotrons and hospitals involved.

3. Results

Four discrete molecular structures were identified in the tissues examined. The fibrillar dimensions, recorded for all samples, were a meridional Bragg *D*-spacing of 65.3 $\pm$ 0.4 nm and a hexagonal packing parameter of 1.41 $\pm$ 0.03 nm. Five or more orders of the low-angle equatorial reflections were fitted to cylindrical arrays in the first-order Bessel function analysis to determine the fibril radius. The average values obtained, 31.4 $\pm$ 1.5 nm for breast cancer patients and 30.9 $\pm$ 1.5 nm for controls, were not significantly different. All samples also exhibited up to 20 orders of a very long equatorial Bragg spacing which corresponds to 353 $\pm$ 3 nm.

The main differences between the four molecular structures are manifested in the presence or absence of sets of rings superimposed on the fibrillar pattern. The presence of fat in the tissue results in wide diffuse rings superimposed on the fibrillar pattern as illustrated in Fig. 3(*a*). Two discrete sets of fine rings were observed in the intensity patterns of the pathological samples. In rare cases, both sets were observed for the same sample. One of these sets was found predominantly in tissues that contained sections of the carcinomatous mass or were taken from areas within 10 mm of the carcinoma. This set of rings indexed onto a spacing of 32.1 $\pm$ 0.5 nm while the other indexed onto a spacing of 43.8 $\pm$ 0.5 nm.

The location of each of these structures in relation to the cancer was deduced from the results obtained for the multiple sample sets and their accompanying histopathology reports. Some typical diffraction intensity patterns for normal and pathological tissues which do not contain fat are shown in Figs. 3(*b*), 3(*c*) and 3(*d*). The location of the structural types relative to the cancer, as observed from the individual multiple sample sets, is shown in Fig. 4.

The percentage content of collagen type III in the fibres was determined as 24% by electrophoresis studies on a number of breast tissue samples.

4. Discussion

The *D*-spacing and hexagonal packing parameters for all breast samples correlate well with values obtained for other fibres with 24% collagen type III content, such as human and porcine heart valves (James *et al.*, 1991). Although the breast might be regarded as a skin appendage, the fibrillar radii obtained for all breast samples were lower than those obtained for skin or heart valves from persons of the same age. However, the average values obtained for both pathological and control breast tissues were statistically the same. A comparison of the values obtained for skin and for breast tissue for various age groups is given in Fig. 5. This graph shows that the

† Aetiology is the sequence of events or changes that lead up to or cause the disorder or disease under investigation. In this case these changes in the collagenous tissue are proemial changes in that they occur before the cancer itself, and are acting like a prelude to the cancer.

average values obtained for all breast tissue is at the higher end of the values obtained by James *et al.* (1998) for foetal tissue. There was a slight variation between the different age groups as can be seen from Fig. 5. A similar variation in this fibril radius has been reported by Lewis *et al.* (2000). However, our study revealed that even greater differences were obtained between the individual samples within each age group (standard deviations for age groups varied from 1 to 2.1 nm for pathological samples and from 0.6 to 2.1 nm for controls). Variations of 0 to 1.9 nm were also obtained between individual samples from the same patient within the multiple sample sets. The slight statistically non-significant difference may be a product of sampling.

The weak signal of the 353 $\pm$ 2 nm equatorial pattern is found in all collagenous connective tissue (James *et al.*, 1993*b*). This spacing is identical to that obtained for the 'chicken wire' lattice branching network formed by the collagen type IV stems emerging from the 7S helical domain, first observed by Timpl *et al.* (1981). Ferguson *et al.* (1992) confirmed the presence of such a lattice in normal breast tissue using specific staining for collagen type IV. Verhoeven *et al.* (1990) have confirmed its presence as associated with periductal elastosis in breast cancer.

While the presence or absence of the wide diffuse ring, Figs. 3(*a*) and 3(*b*), indicates only the presence or lack of fat in the sample, the sets of fine rings that appear in all pathological and some controls are most interesting. These indicate the presence of molecular spatial repeat distances acting over comparatively large intermolecular distances, but randomized in their orientation with respect to the fibrils. The set which corresponds to a spacing of 32.1 $\pm$ 0.5 nm is mainly found in tissues adjacent to the cancer site. This pattern is identical to that found for primordial foetal tendon and skin by James *et al.* (1998). The 32.1 nm spacing is identical to the length of the 7S section of collagen type IV and could result from a disordered array of such helices. Salo *et al.* (1985), using medium from TPA (phorbol ester tumour promoter) treated breast cancer tissue, have reported the presence of a metal-dependent type IV collagenase, which appears to be secreted mainly in latent form. This collagenase cleaves the collagen type IV at specific sites which have been identified in cell cultures from malignant tumours by Fessler *et al.* (1984). The length

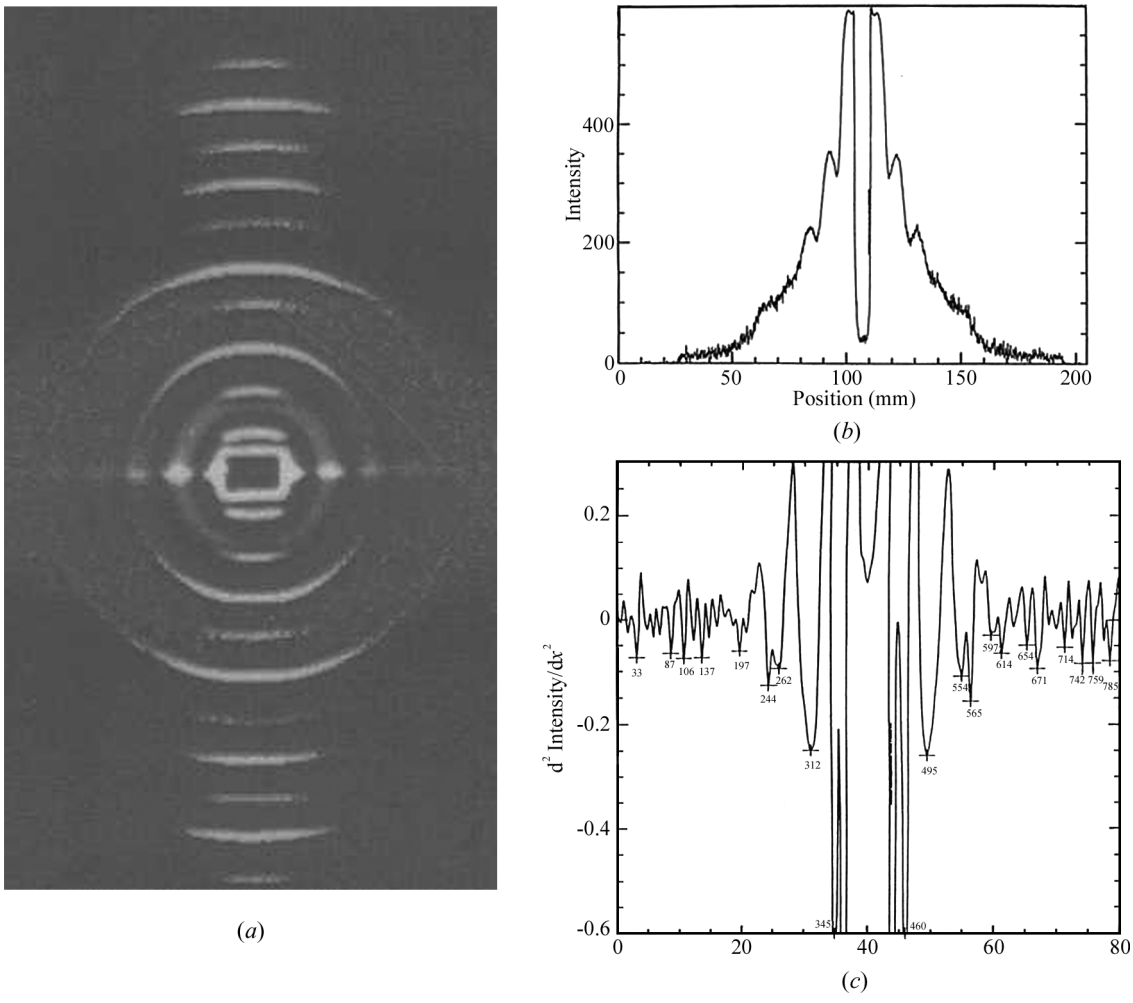

Figure 2
(*a*) A typical low-angle fibre diffraction pattern of normal breast tissue taken with a camera length of 2400 mm. The meridional reflections (vertical) index onto the *D*-spacing of the type I and type III collagen fibrils. In (*b*), a plot of the intensities *versus* position in the equatorial direction, the positions of the stronger peaks are used in the first-order Bessel function analysis to determine the radii of the collagen fibrils. The weak superimposed signal evident at the higher angular positions arises from the 353 nm lattice of collagen type IV. A full description of the measurement of the parameters of this lattice is given by James *et al.* (1993*b*). The positions of the various orders of this large lattice were accurately determined from a plot of the second-order derivative of the intensities, obtained in the synchrotron experiments, with respect to position, (*c*). The pixel readings for a number of the peaks are given on the graph.

of the shorter fragment found by Fessler *et al.* (1984) is 32.1 nm. However, fragmentation of collagen type IV requires a specific pH of 7.5 and the presence of calcium ions, according to the results of Seltzer *et al.* (1976).

The fourth structure is similar to that of foetal tissue in all respects except that the set of rings corresponds to a spacing of 43.8 ± 0.5 nm. Rings with a similar spacing but with differing intensities have been found in the fibre patterns of cartilage and bone and in other diseased tissues where calcium is involved (V. J. James, unpublished data). These rings most probably result from extraneous material bound to the hydroxyl groups, which, from the amino acid sequence (Glanville, 1987), are located at 1/8 intervals along the 'spider legs' of collagen type IV. While these rings might be associated with the laminin-binding foetal-like collagen reported by Pucci-Minafra *et al.* (1993),

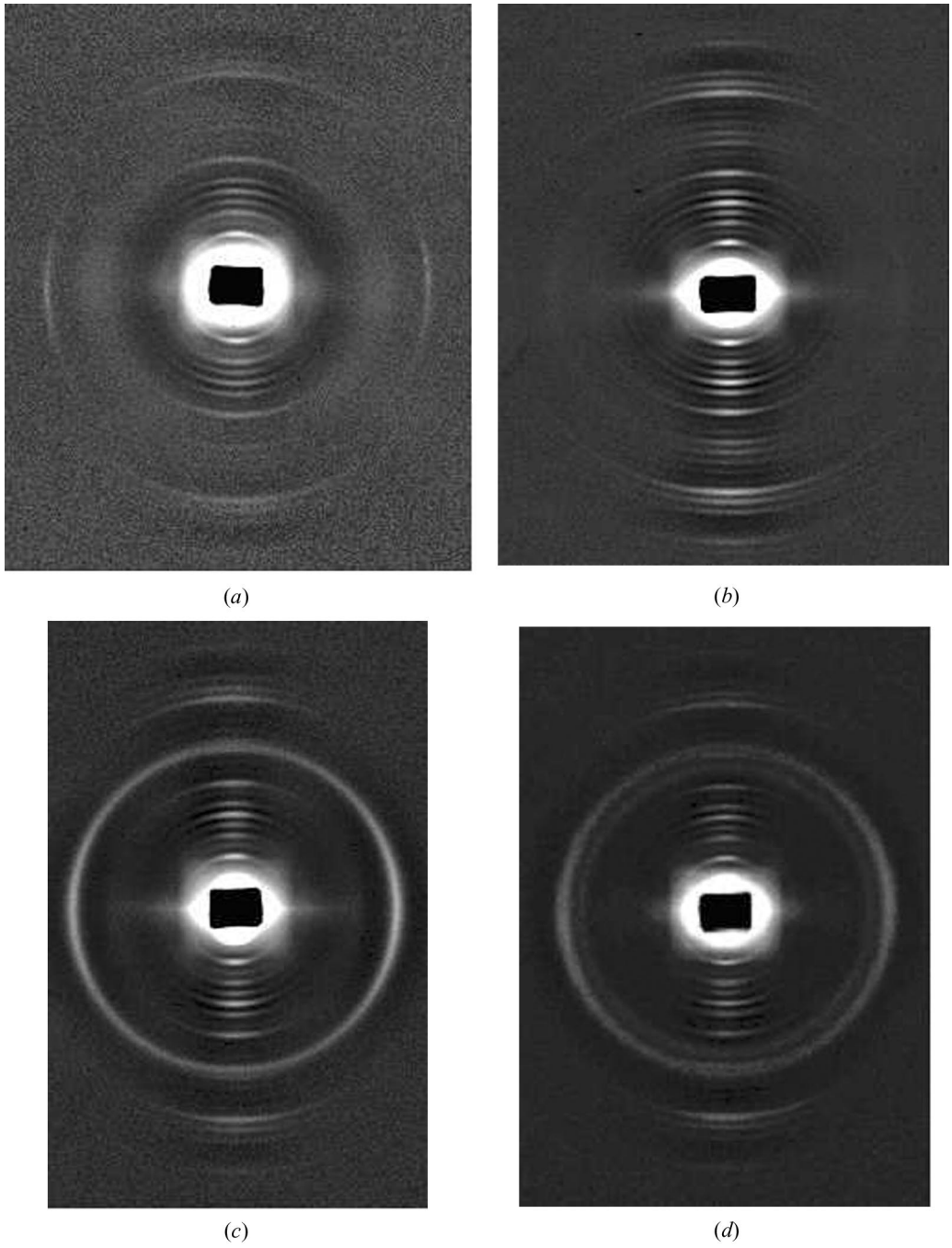

Figure 3
These four fibre diffraction patterns of the breast tissue samples, taken with camera lengths of 600 mm, reveal the four different structures observed with breast carcinoma. (*a*) The pattern obtained for a typical normal 'fibrillar' collagenous breast tissue sample lying parallel to and aligned along a duct. The very wide diffuse ring indicates the presence of fat in this tissue sample. (*b*) The pattern obtained for normal breast tissue from which all fat has been removed. The fibrillar pattern has not altered. (*c*) The fibre diffraction pattern obtained for tissues on sections of ducts which were located adjacent to the tumour. Besides the normal fibrillar pattern, a narrow ring which indexed onto a spacing of 32.1 nm is superimposed onto the normal fibrillar pattern obtained from breast tissue. Some samples showed up to five very weak orders of this lattice. A similar pattern is obtained for undifferentiated embryonic foetal tissue. (*d*) A composite diffraction pattern showing both the ring obtained for foetal tissue and that obtained for foetal-like tissue. Again the fibrillar pattern is the same.

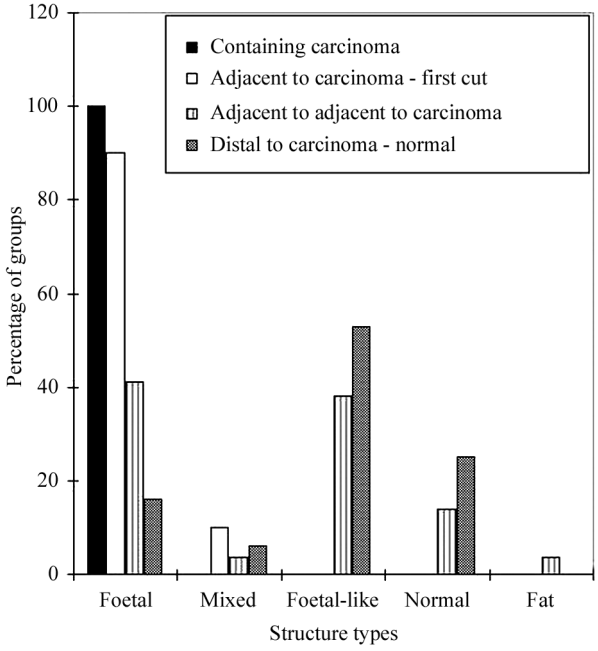

Figure 4
A statistical plot of the distribution of the four structural types relative to the distance of the individual samples from the carcinoma. The graph shows that a foetal structure was obtained for 100% of the samples which contained cancerous material and for 90% of the samples immediately adjacent to these as you move along the duct away from the tumour. Foetal-like tissue was found in the tissue taken further away from the cancer. Very few samples contained rings from both the foetal and foetal-like patterns. Changes were seen in some samples assessed to be normal by histopathology indicating that this method may detect changes not visible in histopathology.

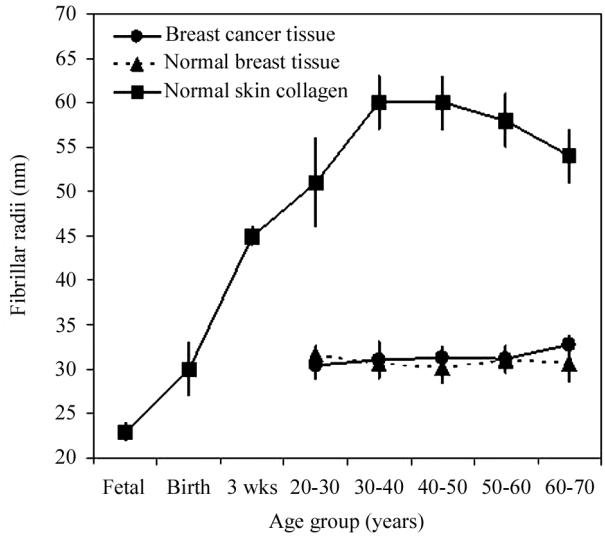

Figure 5
A plot of the fibrillar radii for breast tissue *versus* age. It also includes a distribution of such radii for skin, as obtained from the first-order Bessel function of the equatorial fibre diffraction results from 192 skin samples ranging from foetal to persons over the age of 80. This plot shows that the values obtained for the breast tissue is markedly less than that of skin, even though the breast is virtually a skin appendage. The results indicate that there is no statistical variation between the values obtained for normal and pathological samples from the breast as the variations between the samples of any group are less than the differences observed between the individual samples of that group that were taken from the same breast. The variation with age is also far less than the standard deviations obtained for the set.

the hyaline nature of the collagen as observed in histopathology and the similarities between these diffraction patterns and the diffraction patterns for cartilage would indicate that the bonding material is most probably due to Ca^{++} which is known to be present in the tissue.

Since the number of orders is limited, these rings could also index onto twice this value, *viz.* 87.6 $\pm$ 0.5 nm. This is the length of the longer fragment of collagen type IV found by Fessler *et al.* (1984). Both these possibilities could coexist and both have a statistical R^2 value of 0.999 for the best least-squares fit.

5. Conclusion

These studies have been conducted on a large number of samples and also included a large number of multiple samples from 30 individuals. The findings have demonstrated three major structural changes in the breast which are associated with and precede the development of breast carcinoma. These changes are related to the cleavage of collagen type IV, the final stage of which is foetal tissue.

The locations of the foetal tissue and the intermediate molecular changes of the stroma have shown that the foetal tissue is found adjacent to the tumour. The foetal-like tissue lies between the foetal tissue and the normal tissue, found distal from the tumour. There is a virtual absence of fat in some of the normal tissue. While this study examines ductal and lobular infiltrative and non-infiltrative cancers, further studies are under way to ascertain whether similar or different structural changes also occur in different subtypes of breast carcinoma. Since an evaluation of the percentage of foetal collagen against tumor grade also fell outside the parameters of this experiment and, as a consequence, these details were not included in the histopathology results requested, the parameters of our continuing studies have been widened to include such an evaluation.

The author wishes to acknowledge the generous support of the Photon Factory for the use of this facility and for the assistance provided for this project, No. 93G031, and to the BioCAT facility of the Advanced Photon Source which is supported by the US Department of Energy, Basic Energy Sciences, Office of Science, under contract No. W-31-109-ENG-38. BioCAT is a National Institutes of Health-supported Research Center, RR-08630. Financial support from the Australian National Beamline Facility is acknowledged. The ANBF is funded by a consortium comprising the ARC, DITARD, ANSTO, CSIRO, ANU and the UNSW. The author would also like to acknowledge financial support from the Australian Research Council, Quota International Inc., the Ladies' Auxiliary of the Camden Valley Way Golf Club and private donations to the UNSW Physics Cancer Research Fund; assistance with histopathology from the late Dr James Halley, Prince of Wales Hospital, Dr John O'Brien, O'Brien Pathology, Randwick NSW, Dr Michael Billous, Westmead Hospital; valuable discussions regarding the pathology of the samples with Dr B. Cook, Anatomical Pathology, Prince of Wales Hospital, Sydney; valuable assistance with the production of the script from Professor John Kearsley, Cancer Care Centre, St George Hospital, Kogarah, Dr Eugenie Willis, Portland, Oregon, Dr David Cookson, ChematCARS, APS; and the provision of samples by Westmead Hospital (Sydney), Royal Prince Alfred Hospital (Sydney), Royal North Shore Hospital (Sydney) and the Breast Cancer Clinic of All Russia. The author would also like to thank Dr D. Chan, Royal Children's Hospital Melbourne, for help with the electrophoresis, and the Electron Microscopy Unit at the University of Queensland for help with the electron microscopy.

References

Ferguson, J. E., Schor, A. M., Howell, A. & Ferguson, M. W. J. (1992). *Cell Tissue Res.* **268**, 167–177.

Fessler, L. I., Duncan, K. G., Fessler, J. H., Salo, T. & Tryggvason, K. (1984). *J. Biol. Chem.* **259**, 9783–9789.

Glanville, R. W. (1987). *Structure and Function of Collagen Types*, United Kingdom ed., edited by R. Mayne & R. E. Burgeson, pp. 43–73. New York: Academic Press.

IRAF Programming Group (1986). *IRAF. An Image Reduction and Analysis Facility.* National Optical Astronomy Observatories, Tucson, AZ, USA.

James, V. J., McConnell, J. F. & Amemiya, Y. (1993*a*). *Photon Factory Activity Report*, Vol. 11, p. 346. Photon Factory, Tsukuba, Japan.

James, V. J., McConnell, J. F. & Amemiya, Y. (1993*b*). *Biochim. Biophys. Acta*, **1202**, 305–308.

James, V. J., McConnell, J. F. & Amemiya, Y. (1998). *Biochim. Biophys. Acta*, **1379**, 282–288.

James, V. J., McConnell, J. F. & Capel, M. (1991). *Biochim. Biophys. Acta*, **1078**, 19–22.

Lewis, R. A., Rogers, K. D., Hall, C. J., Towns-Andrews, E., Slawson, S., Evans, A., Pinder, S. E., Ellis, I. O., Boggis, C. R. M., Hufton, A. P. & Dance, D. R. (2000). *J. Synchrotron Rad.* **5**, 348–352.

Pucci-Minafra, I., Luparelli, C. A., Basirico, L., Minafra, S., Franc, S., Yakovlev, L. & Shoshan, S. A. (1993). *Biochemistry*, **32**, 7421–7427.

Salo, T., Tureenniemi-Hujanen, T. & Tryggvason, K. (1985). *J. Biol. Chem.* **260**, 8526–8531.

Seltzer, J. L., Welgus, H. G., Jeffrey, J. J. & Eizen, A. Z. (1976). *Arch. Biochem. Biophys.* **173**, 355–361.

Timpl, R., Wiedemann, H., Van Delden, V., Furthmayr, H. & Kühn, K. A. (1981). *Eur. Biochem.* **120**, 203–211.

Van Hilst, M. (1990). *SAO Image. An Image Display Utility.* Smithsonian Astrophysics Observatories, Cambridge, MA, USA.

Verhoeven, D., Bourgeois, N., Noël, A., Foidart, J. M. & Buyssens, N. (1990). *J. Histochem. Cytochem.* **38**, 245–255.

 Received 24 September 2001 • Accepted 23 January 2002